JOURNAL OF SOLID STATE CHEMISTRY 24, 11–19 (1978)

Thermodynamics of $Mg_yU_{1-y}O_{2+x}$ by EMF Measurements. I. Properties at High Magnesium Concentrations

TAKEO FUJINO, JUN TATENO, AND HIROAKI TAGAWA

Chemistry Division, Japan Atomic Energy Research Institute, Tokai-mura, Ibaraki, Japan

Received July 11, 1977

Phase stability and thermodynamic properties of a solid solution, $Mg_yU_{1-y}O_{2+x}$, have been investigated at high magnesium concentrations. The lattice constant of this cubic solid solution varies differently with x in the two regions of positive and negative x values. The relation between the lattice constant and the composition was determined in the respective regions. Solid-state emf measurements on $Mg_yU_{1-y}O_{2+x}$ revealed that both partial molar entropy and enthalpy of oxygen are temperature independent in the experimental range 700 ~ 1050°C and that $-\Delta\bar{S}_{O_2}$ and $-\Delta\bar{H}_{O_2}$ increase with x and y of $Mg_yU_{1-y}O_{2+x}$. Least-squares calculations showed that $-\Delta\bar{S}_{O_2}$ and $-\Delta\bar{H}_{O_2}$ could be expressed as logarithmic functions of x and y. The negative partial molar free energy, $-\Delta\bar{G}_{O_2}$, obtained by the $\Delta\bar{S}_{O_2}$ and $\Delta\bar{H}_{O_2}$ formulas was found to decrease with temperature more rapidly for the solid solutions of larger y values, which indicates the greater effect of divalent magnesium on the thermodynamic properties of $Mg_yU_{1-y}O_{2+x}$.

Introduction

It is known that several metal ions can be incorporated in UO_2 crystal forming substitutional solid solutions, $M_yU_{1-y}O_{2+x}$, where M is the metal ion. In these solid solutions, impurity ions interact with the uranium and oxygen ions of the host crystal, which causes change in thermodynamic properties from those of UO_{2+x}. Great interest attaches to the comparison of the thermodynamic data for $M_yU_{1-y}O_{2+x}$ in the group of the foreign metal valency, i.e., M^{1+}, M^{2+}, M^{3+}, etc.

Divalent magnesium forms a solid solution of $Mg_yU_{1-y}O_{2+x}$ in rather a wide range of the magnesium concentrations with y values between 0 and 0.33 (*1*, *2*) in spite of the fact that the ionic radius of Mg^{2+} (r = 0.66 Å (*3*)) is considerably smaller than that of U^{4+} (r = 0.97 Å (*3*)). The solid solution has a cubic fluorite structure in which the magnesium ions statistically occupy the uranium lattice sites and the excess oxygen ions corresponding to x in $Mg_yU_{1-y}O_{2+x}$ occupy the interstitial sites (*4*).

There have been many reports (*1*, *5–8*) concerning the preparation and properties of the $Mg_yU_{1-y}O_{2+x}$ phase. However, inconsistencies are seen among them with regard to the stable temperature and the composition range of the compound. In our previous paper (*2*), the $Mg_yU_{1-y}O_{2+x}$ ($0 \leqq y \leqq 0.33$) was prepared in single phase by the reaction of magnesium uranates ($MgUO_4$, MgU_3O_{10}) and UO_2 in the streams of helium at 1100 ~ 1350°C. This means that the oxygen partial pressure in the helium atmosphere was just in the pressure range of the single phase. But for an extensive discussion of the stability of an $Mg_yU_{1-y}O_{2+x}$ solid solution, it is required that the thermodynamic properties be known over the system.

We describe here the thermodynamic properties of the $Mg_yU_{1-y}O_{2+x}$ measured by the solid-state galvanic cell method. Partial molar

0022-4596/78/0241-0011$02.00/0

free energies, enthalpies, and entropies of oxygen were obtained at temperatures between 650 and 1050°C with the y values mainly over 0.05. The data at low magnesium concentrations will be presented in a later paper. The thermodynamic values are expressed as functions of temperature and composition of the solid solution, and the agreement between measured and theoretically calculated entropies is briefly discussed.

Experimental

1. Preparation of $Mg_yU_{1-y}O_{2+x}$

The $Mg_yU_{1-y}O_{2+x}$ samples with high magnesium concentrations were prepared by reaction in streams of helium. The method is essentially the same as that reported previously (*2*): Calculated amounts of MgU_3O_{10} and UO_2 were mixed in an agate mortar for several y values below 0.33 (y = 0.01, 0.02, 0.05, 0.10, 0.15, 0.20, and 0.25). In order to obtain intimate mixtures which result in the formation of homogeneous $Mg_yU_{1-y}O_{2+x}$ compounds, mixing was performed by diluting the starting materials with UO_2 stepwise. For example, the y = 0.15 mixture was obtained by mixing calculated amounts of the y = 0.20 mixture and UO_2, and the y = 0.10 mixture by mixing calculated amounts of the y = 0.15 mixture above and UO_2, and so on. Reaction was performed after the mixture was pressed into pellets of 10-mm diameter.

To obtain an $Mg_yU_{1-y}O_{2+x}$ compound with low x values, mixtures were heated under vacuum. In this case, the reaction was carried out under a high vacuum of $<4 \times 10^{-5}$ Torr at temperatures of 1300 ~ 1550°C for 20 hr.

In a series of experiments carried out to examine the solubility of magnesium in the $x <$ 0 range, hydrogen reduction of the solid solutions was conducted at 1300°C.

2. Determination of Oxygen in $Mg_yU_{1-y}O_{2+x}$

The x value of the $Mg_yU_{1-y}O_{2+x}$ was determined by the compound addition method (*9*). The method consists of mixing of an $Mg_yU_{1-y}O_{2+x}$ sample with $MgUO_4$ or Sr_2UO_5 followed by heating at 700 ~ 900°C in air to produce the uranates in which all the uranium atoms have a formal charge of +6. The x value can be calculated from the weight difference before and after the heating. The estimated error in x was ± 0.002, which is smaller by one order of magnitude than that calculated by the usual cerimetric method. The x value was related to the cubic lattice constant of the compound in the respective regions of $x \geqq 0$ and $x < 0$. The determination of the oxygen in the sample was performed mainly by these equations after the relations were established. The lattice constant from the Debye–Scherrer photograph, which was taken by a Norelco 114.6-mm camera, could be obtained with the capillary containing less than 100 mg of powder sample from the edge of the pellet which was subjected to emf measurements.

3. Measurement of Electromotive Force

The solid cell employed was of the type

$$\text{Ni, NiO/solid electrolyte/}Mg_yU_{1-y}O_{2+x}, \quad (1)$$

where the solid electrolyte was a solid solution of 0.15 CaO and 0.85 ZrO_2. The schematic drawing of the cell is shown in Fig. 1. The three pellets of (Ni, NiO), solid electrolyte, and $Mg_yU_{1-y}O_{2+x}$ were sandwiched between two Pt disks which were welded to Pt wires for electrical contact. The effect of contact resistance was minimized by putting a Pt weight of about 20 g on them. After the pellets were placed in position, the system was evacuated to $<10^{-5}$ Torr for over 2 hr. Then the stopcock connected to the vacuum pump was closed, and helium gas was introduced into the system. The helium used was a gas of 99.999% purity passed through a liquid nitrogen trap and then through a hot Ni oxygen collector (*10*), in which measurements of emf were carried out with a flow rate of ~5 ml/min.

For having (Ni, NiO) pellets, finely divided Ni metal of 99.998% purity from Halewood Chemicals Ltd. was dissolved in nitric acid,

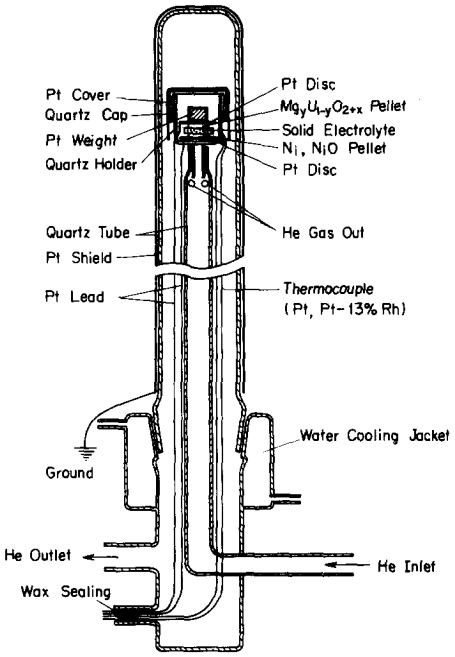

FIG. 1. Schematic of the solid cell; Ni, NiO/solid electrolyte/$Mg_yU_{1-y}O_{2+x}$.

and then nickel carbonate precipitate was obtained by adding ammonium carbonate to the solution. The nickel carbonate was converted into NiO by the heat at 900°C in air. Approximately the same weights of Ni and NiO were mixed, and pressed into cylindrical pellets of 10-mm diameter with ~2-mm thickness. The solid electrolyte pellets of 15-mm diameter were purchased from Nippon Kagaku Togyo Co. Ltd., the purity of which was $SiO_2 < 0.5\%$, $Al_2O_3 < 0.3\%$, $TiO_2 < 0.3\%$, $Fe_2O_3 < 0.1\%$.

The temperature fluctuation of the cell was within 0.2% in an automatically controlled Kanthal resistance furnace. The electrical noise from the furnace was eliminated by a Pt shield outside the quartz tube. The temperature gradient around the cell was checked by measuring the emf of a cell

Ni, NiO/solid electrolyte/Ni, NiO, (2)

in which the emf was found to be less than 2 mV at temperatures between 700 and 1050°C,

The measurements of emf were carried out with a potentiometer and a Keithley high-impedance ($>10^{14}\ \Omega$) microvoltmeter. In order to ascertain that no systematic deviations from the reasonable emf values were seen in a cell of this type, the values were measured for a cell

Ni, NiO/solid electrolyte/Cu, Cu_2O. (3)

The emf data obtained were in accord with those of Markin and Bones (*11*) within ±2 mV at temperatures 700 ~ 900°C, so that

$$\Delta\bar{G}_{O_2}(\text{Ni, NiO}) = -113300 + 41.5T\,(\text{K}) \quad (\text{cal}_{th}\,\text{mole}^{-1})^1 \qquad (4)$$

was used according to the assessment by them as the partial molar free energy for the reaction $2Ni + O_2 = 2NiO$.

4. *Calculation of* $\Delta\bar{G}_{O_2}$, $\Delta\bar{H}_{O_2}$, $\Delta\bar{S}_{O_2}$

The partial molar free energy of oxygen for the sample was calculated by the relation

$$\Delta\bar{G}_{O_2}(Mg_yU_{1-y}O_{2+x}) = 4EF + \Delta\bar{G}_{O_2}(\text{Ni, NiO}), \qquad (5)$$

where E is the emf and F is the Faraday constant (*12*) (23 062 $\text{cal}_{th}\ V^{-1}\ \text{equiv}^{-1}$). The $\Delta\bar{G}_{O_2}$ values obtained were found to vary approximately linearly with temperature. Therefore, the negative partial molar entropy of oxygen, $-\Delta\bar{S}_{O_2}$, was worked out as the least-squares calculated slope, $\Delta(\Delta\bar{G}_{O_2})/\Delta T$, in the linear region. The least-squares calculations in this paper were carried out by a FACOM 230-75 computer. The partial molar enthalpy of oxygen, $\Delta\bar{H}_{O_2}$, was obtained by the equation

$$\Delta\bar{H}_{O_2} = \Delta\bar{G}_{O_2} + T\cdot\Delta\bar{S}_{O_2}. \qquad (6)$$

Results and Discussion

1. *Lattice Constant as a Function of Composition*

The lattice constant of the cubic fluorite type solid solution, $Mg_yU_{1-y}O_{2+x}$, varies fairly

[1] Throughout this paper $\text{cal}_{th} = 4.184$ J.

TABLE I

ANALYSIS OF THE COMPOSITION OF $Mg_yU_{1-y}O_{2+x}$ IN RELATION WITH LATTICE CONSTANT

No.	y	x (By compound addition method)	Lattice constant (Å)	x (From Eq. (7) or Eq. (8))
1	0.05	0.021	5.4454	−0.004
2	0.05	0.208	5.4239	0.204
3	0.10	0.140	5.4021	0.142
4	0.10	0.156	5.4012	0.152
5	0.15	−0.025	5.4135	−0.038
6	0.15	0.058	5.3806	0.072
7	0.20	0.044	5.3547	0.050
8	0.25	−0.075	5.3815	−0.071
9	0.25	0.005	5.3305	0.006
10	0.33	−0.006	5.2823	0.054

largely with the compositions x and y. Although we have previously presented an equation of lattice constant, a_0, as linear functions of x and y (*2*), the relation was reinvestigated in order to obtain x values by the equation with more accuracy from y and a_0. The results are tabulated in Table I. It was found in the present study that the variation of the lattice constant was better expressed by the introduction of a small correction term, $0.055xy$, for the $x \geqq 0$ region. The least-squares calculation revealed that the lattice constant follows the equations

$$a_0\ (\text{Å}) = 5.4704 - 0.0940x - 0.5577y + 0.055xy \quad (\text{for } x \geqq 0), \tag{7}$$

$$a_0\ (\text{Å}) = 5.4704 - 0.7095x - 0.5577y \quad (\text{for } x < 0). \tag{8}$$

The factor 0.5577 should be common in order that the above two equations are consistent at $x = 0$. In Eq. (7), the coefficient (0.0940) of the second term was taken from the work by Nickel (*13*) for UO_{2+x}. The fact that the a_0 variation is suitably described by this coefficient can be interpreted as indicating the similar behavior of the interstitial oxygen in these two compounds. On the other hand, as is seen in Eq. (8), the lattice constant increases with a far greater rate (0.7095) with the formation of oxygen vacancy in the $x < 0$ region.

2. *Single-Phase Region of $Mg_yU_{1-y}O_{2+x}$*

The single-phase region of $Mg_yU_{1-y}O_{2+x}$ for $x \geqq 0$ was examined in our previous paper (*2*), but it may be worthwhile to consider briefly its oxygen pressure dependence.

As reviewed by Keller (*14*), the single-phase region under 0.21-atm oxygen pressure (*15*, *16*) is above ~1200°C, but under $<10^{-4}$-Torr oxygen pressure it falls to ~1000°C. Therefore, the low-temperature limit of the equilibrium single-phase region is inferred to be much lowered under pressure of less than 10^{-7} Torr where the galvanic cell measurements were carried out. Experiments, in fact, showed that the almost-linear emf vs temperature relationship held from 1050°C to around 700°C. Between 600 and 700°C, discontinuities often appeared in the emf curves. These might be attributed to the phase change at first sight, but if it is taken into account that reliable emf data cannot be obtained below ~600°C, the origin remains ambiguous.

The stability range of $Mg_yU_{1-y}O_{2+x}$ with negative x was examined by reaction in hydrogen streams at 1300°C. Figure 2 shows

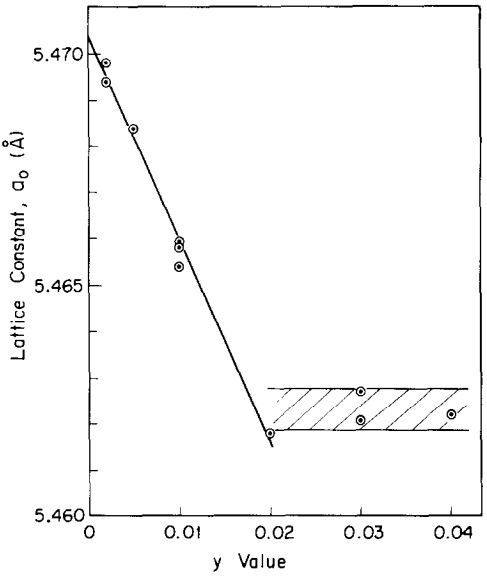

FIG. 2. Solubility of magnesium when heated in hydrogen streams at 1300°C.

the variation of the cubic lattice constant, a_0, with magnesium content. It is seen from the figure that the solubility of magnesium under the above condition is $y = 0.02$ and that the slope in the single-phase region of the solid solution is −0.445, which is in good agreement with the values of Ainscough and Rigby (*17*) (−0.413) and Anderson and Johnson (*18*) (−0.446). According to Ainscough and Rigby, the slope is not changed by the oxygen partial pressure surrounding the solid system from undiluted hydrogen to a 67% H_2– 33% CO_2 gas mixture. The slope −0.445 in this work means that the composition is $Mg_yU_{1-y}O_{2-0.1588y}$ by Eq. (8), which in turn indicates that the mean valency of uranium is $(4 + 1.6824y/(1-y))$. It is known that the increase of uranium valency is less than 2 (1.6824) by the incorporation of one magnesium(II) ion in solid solution; i.e., the lower limit of x increases negatively with increasing values of y. This may explain the fact that $Mg_yU_{1-y}O_{2+x}$ with $x < 0$ is comparatively easily produced if y is not small. The above-mentioned is, however, the boundary composition. Therefore, if the partial pressure of oxygen is lower than that of a compound with a certain y value, because oxygen can no longer be removed, the solid solution might reach equilibrium with that pressure by depositing a part of the magnesium as magnesium oxide. This is, we believe, the reason why the solubility of magnesium is small in a highly reducing atmosphere.

3. *Thermodynamic Values*

Figure 3 represents plots of partial molar free energy of oxygen, $-\Delta\bar{G}_{O_2}$, as a function of temperature for three typical specimens of $Mg_yU_{1-y}O_{2+x}$. The $-\Delta\bar{G}_{O_2}$ values were obtained from emf by Eq. (5). For having constant emf values, measurements were carried out after a certain standing time which is varied from ~0.5 to ~2 hr at 1000 and 700°C, respectively. It is seen from the figure that no hysteresis loops are observed in cooling and heating processes and that the variation of experimental points is almost linear above 700°C, which indicates that the partial molar enthalpy and entropy are temperature independent in this range.

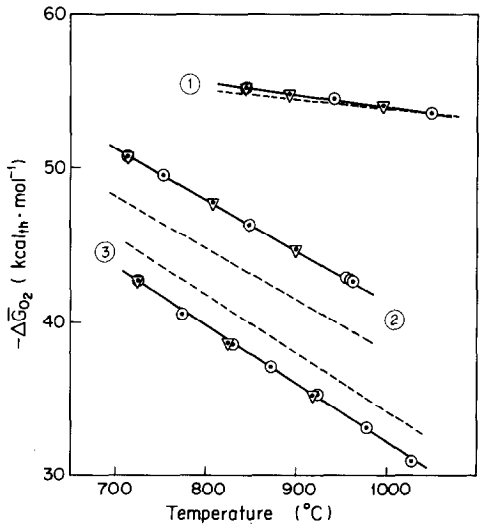

FIG. 3. Example showing linearity and attainment of electrochemical equilibrium with no hysteresis loops: (1) No. 1 sample in Table II; (2) No. 13 sample; (3) No. 17 sample; ⊙ cooling process; △ heating process; —— experimental curve; −−− least-squares curve.

TABLE II

THERMODYNAMIC DATA FOR $Mg_yU_{1-y}O_{2+x}$

No.	y	x	$-\Delta\bar{H}_{O_2}$(obsd) (kcal$_{th}$/mole)	$-\Delta\bar{H}_{O_2}$(calcd) (kcal$_{th}$/mole)	$-\Delta\bar{S}_{O_2}$(obsd) (e.u./mole)	$-\Delta\bar{S}_{O_2}$(calcd) (e.u./mole)
1	0	0.0214	63.6	61.6	7.6	6.1
2	0	0.0339	66.4	64.2	11.2	10.7
3	0	0.0462	66.6	66.0	12.1	13.8
4	0	0.0685	69.4	68.3	16.0	17.8
5	0	0.0874	71.5	69.6	18.7	20.2
6	0	0.1060	73.6	70.8	21.6	22.2
7	0.01	−0.001	65.0	67.1	15.3	9.0
8	0.02	−0.006	70.3	70.9	19.0	15.3
9	0.05	0.045	75.7	77.3	22.2	28.2
10	0.05	0.055	75.6	77.5	23.2	28.7
11	0.05	0.208	81.2	79.6	36.7	34.4
12	0.10	−0.006	80.1	80.4	22.1	32.4
13	0.10	0.029	81.7	80.7	31.6	33.5
14	0.10	0.076	86.8	81.2	37.0	34.8
15	0.10	0.144	89.9	81.7	43.4	36.5
16	0.10	0.161	93.3	81.9	45.5	36.9
17	0.10	0.194	80.2	82.1	37.6	37.6
18	0.15	0.013	92.1	82.9	41.8	36.9
19	0.15	0.068	82.9	83.2	36.3	38.0
20	0.15	0.070	78.5	83.2	32.6	38.1
21	0.15	0.071	85.7	83.2	39.0	38.7
22	0.20	−0.050	80.9	84.2	26.3	38.6
23	0.20	−0.043	83.3	84.2	33.6	38.7
24	0.20	−0.031	87.2	84.3	42.8	39.0
25	0.20	−0.001	84.3	84.4	42.6	39.5
26	0.20	0.014	94.5	84.5	51.3	39.7
27	0.20	0.050	94.3	84.7	47.6	40.3
28	0.25	−0.016	89.4	85.6	35.2	41.5
29	0.25	−0.009	80.4	85.7	35.9	41.6
30	0.25	−0.003	91.2	85.7	43.8	41.7
31	0.25	0.016	77.2	85.8	30.6	41.9
32	0.25	0.066	83.8	86.0	45.4	42.6
33	0.25	0.170	85.0	86.4	45.6	43.8
34	0.25	0.274	87.8	86.7	48.0	44.9
35	0.33	−0.049	88.6	87.2	44.1	44.0

Thermodynamic data for $Mg_yU_{1-y}O_{2+x}$ are given in Table II. The observed values are shown in columns 4 and 6 of the table. Although scattering is not small, the values of $-\Delta\bar{H}_{O_2}$ and $-\Delta\bar{S}_{O_2}$ increase with increasing x and y. Least-squares calculations were performed with the data of Table II to express, first, $\Delta\bar{S}_{O_2}$ as functions of x and y. The equation

$$\Delta\bar{S}_{O_2} = -10.03 \ln (x + 2.985y) - 44.66 \quad \text{(e.u. mole}^{-1}\text{)} \tag{9}$$

was obtained. The adoption of the logarithmic function and linear argument of x and y may be justified by the fact that many theoretical considerations of $\Delta\bar{S}_{O_2}$ of UO_{2+x} have resulted in the logarithmic form (*19*) and that both x and y values are small compared with 1. The $-\Delta\bar{S}_{O_2}$ values calculated by Eq. (9) are shown in column 7 of the table. The experimental data and the least-squares $-\Delta\bar{S}_{O_2}$ are represented in Fig. 4 against x in $Mg_yU_{1-y}O_{2+x}$ for several fixed y ($y = 0$, 0.05, 0.1, 0.15, 0.2, and

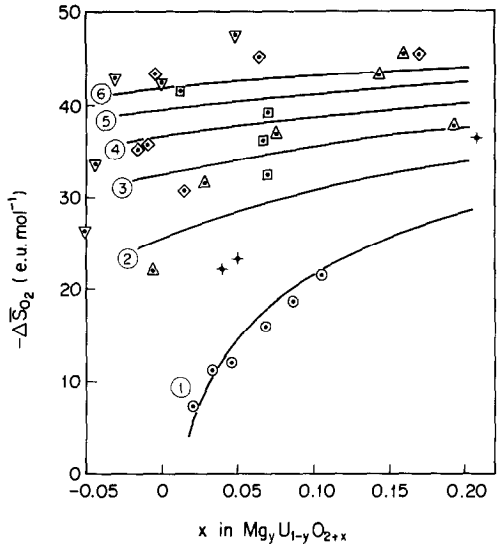

FIG. 4. Plots of negative partial molar entropy of oxygen against x in $Mg_yU_{1-y}O_{2+x}$ at various y; observed points: ⊙ $y = 0$, + $y = 0.05$, △ $y = 0.1$, ⊡ $y = 0.15$, ▽ $y = 0.2$, ◇ $y = 0.25$; least-squares curves: (1) $y = 0$, (2) $y = 0.05$, (3) $y = 0.1$, (4) $y = 0.15$, (5) $y = 0.2$, (6) $y = 0.25$.

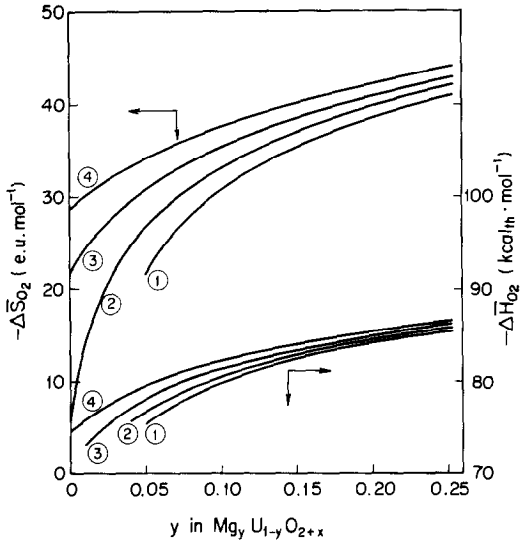

FIG. 5. Variation of least-squares-calculated $-\Delta\bar{S}_{O_2}$ and $-\Delta\bar{H}_{O_2}$ with y in $Mg_yU_{1-y}O_{2+x}$; (1) $x = -0.05$, (2) $x = 0.02$, (3) $x = 0.1$, (4) $x = 0.2$.

0.25). The observed entropy for UO_{2+x} is seen to be consistent with the published data (*11*, *19–22*), and the curve for UO_{2+x} agrees well with the observed values. However, the agreement of the curves with the observed points is not clear in the case of $Mg_yU_{1-y}O_{2+x}$, because of the scatter of the points. The variation of the least-squares $-\Delta\bar{S}_{O_2}$ with y for several fixed x ($x = -0.05$, 0.02, 0.1, and 0.2) is depicted in Fig. 5. It is known that the effect of y (magnesium) on $-\Delta\bar{S}_{O_2}$ is larger than that of x (oxygen).

Least-squares calculations on partial molar enthalpy, $\Delta\bar{H}_{O_2}$, gave the empirical formula

$$\Delta\bar{H}_{O_2} = -5.735 \ln(x + 5.755y) - 83.62 \quad (\text{kcal}_{th}\ \text{mole}^{-1}). \qquad (10)$$

As input data, all values of y, x, and $-\Delta\bar{H}_{O_2}$(obsd) in Table II were used. The $-\Delta\bar{H}_{O_2}$ values calculated by Eq. (10) are shown in column 5. The plots of experimental data and the least-squares values of $-\Delta\bar{H}_{O_2}$ are given in Fig. 6 for various y ($y = 0$, 0.05, 0.1, 0.15, 0.2, and 0.25). The observed values of $-\Delta\bar{H}_{O_2}$ for UO_{2+x} are in agreement with the reported data (*11*, *19–22*), and the least-squares curve for UO_{2+x} is seen to follow the observed points satisfactorily. For

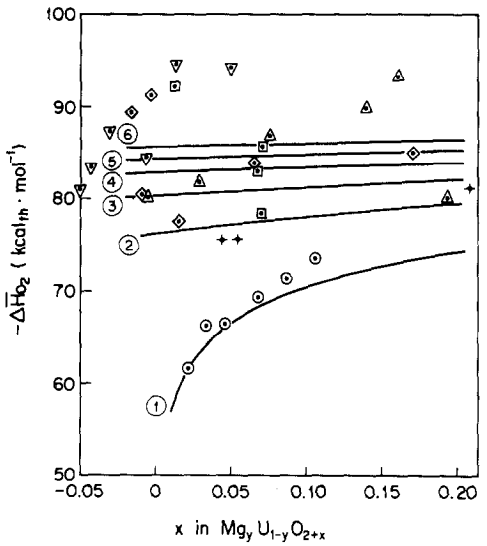

FIG. 6. Plots of negative partial molar enthalpy of oxygen against x in $Mg_yU_{1-y}O_{2+x}$ at various y; observed points: ⊙ $y = 0$, + $y = 0.05$, △ $y = 0.1$, ⊡ $y = 0.15$, ▽ $y = 0.2$, ◇ $y = 0.25$; least-squares curves: (1) $y = 0$, (2) $y = 0.05$, (3) $y = 0.1$, (4) $y = 0.15$, (5) $y = 0.2$, (6) $y = 0.25$.

$Mg_yU_{1-y}O_{2+x}$, however, the comparison is difficult to make because of the large scattering of the data, but the curve for $y = 0.05$ is at least consistent. In spite of linear dependence of emf on temperature for each sample, the values of $-\Delta\bar{H}_{O_2}$ scatter with the sample. These phenomena are also seen in the reports for UO_{2+x} (*19*), where the discrepancy of ~10 $kcal_{th}$ $mole^{-1}$ seems to be unavoidable in $\Delta\bar{H}_{O_2}$. The reason that the error is augmented in the three-component compound, $Mg_yU_{1-y}O_{2+x}$, is still not clear.

The variation of partial molar enthalpy with y is shown in Fig. 5. The fact that $\Delta\bar{H}_{O_2}$ and $\Delta\bar{S}_{O_2}$ increase negatively with increasing x and/or y is also seen in the reports for $La_yU_{1-y}O_{2+x}$ (*23*), $Y_yU_{1-y}O_{2+x}$ (*24*), and $Th_yU_{1-y}O_{2+x}$ (*20*). It is characteristic in $Mg_yU_{1-y}O_{2+x}$ that $-\Delta\bar{H}_{O_2}$ and $-\Delta\bar{S}_{O_2}$ increase steeply with x or y in the range of small x and y, which is also observed in $La_yU_{1-y}O_{2+x}$ (*23*). Moreover, the effect of y on $-\Delta\bar{H}_{O_2}$ as well as on $-\Delta\bar{S}_{O_2}$ is greater in $Mg_yU_{1-y}O_{2+x}$ and $La_yU_{1-y}O_{2+x}$ than in $Th_yU_{1-y}O_{2+x}$.

In our earlier paper (*2*), we presented a statistical model showing that part of the uranium atoms in $Mg_yU_{1-y}O_{2+x}$ are oxidized to U(V) not only by excess oxygen in the interstitial position of the fluorite lattice but also by magnesium ions substituted in the uranium site of the crystal. By counting the number of arrangement of these ions,

$$\Delta\bar{S}_{O_2} = -2R \cdot \ln \frac{x}{1-x} - 4R \cdot \ln \frac{2x+2y}{1-2x-3y} + Q \qquad (11)$$

was obtained. Because the above equation is for the dilute defect system where the oxidized U(V) does not interact with the other ions, the applicable range of this equation is restricted to small x and y. Comparison of Eqs. (9) and (11) reveals that $\Delta\bar{S}_{O_2}$ values calculated by Eq. (11) are fairly well in accord with those calculated by Eq. (9) if x and y are both less than 0.05 and Q is $-45 \sim -47$ e.u. $mole^{-1}$.

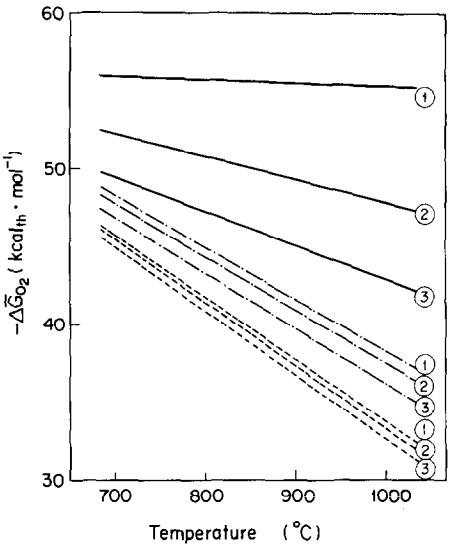

FIG. 7. Variation of least-squares-calculated $-\Delta\bar{G}_{O_2}$ with temperature for various x and y of $Mg_yU_{1-y}O_{2+x}$; (1) $x = 0.02$, (2) $x = 0.05$, (3) $x = 0.1$; ——, $y = 0$; —·—·—, $y = 0.1$; – – –, $y = 0.2$.

The calculated partial molar free energy of oxygen is illustrated as dashed lines in Fig. 3 for three cases. It is mainly due to the scattering of $\Delta\bar{H}_{O_2}$ (obsd) that agreement is not always good between observed and calculated $-\Delta\bar{G}_{O_2}$ values. The variation of $-\Delta\bar{G}_{O_2}$ (calcd) with temperature is shown in Fig. 7 for various x and y values ($x = 0.02$, 0.05, and 0.1; $y = 0$, 0.1, and 0.2). It is clear from the curves that $-\Delta G_{O_2}$ decreases with increasing x and y, but the effect of x is rather small in the range of large y ($y = 0.2$). Another trend is that the decreasing rate of $-\Delta\bar{G}_{O_2}$ with temperature is enhanced for larger y values, and from these facts the great effect of divalent magnesium in UO_2 lattices on thermodynamic values can be indicated.

References

1. S. KEMMLER-SACK AND W. RÜDORFF, *Z. Anorg. Allg. Chem.* **354**, 255 (1967).
2. T. FUJINO AND K. NAITO, *J. Inorg. Nucl. Chem.* **32**, 627 (1970).
3. L. H. AHRENS, *Geochim. Cosmochim. Acta* **2**, 155 (1952).
4. T. FUJINO, *J. Inorg. Nucl. Chem.* **34**, 1563 (1972).

5. H. R. HOEKSTRA AND J. J. KATZ, *J. Amer. Chem. Soc.* **74**, 1683 (1952).
6. H. HOEKSTRA AND S. SIEGEL, *in* "Proceedings of the International Conference on the Peaceful Uses of Atomic Energy, Geneva 1955," Vol. 7, p. 394 (1956).
7. E. A. IPPOLITOVA, Yu. P. SIMANOV, L. M. KOVBA, G. P. POLUNINA, AND I. A. BEREZNIKOVA, *Radiokhimiya* **1**, 660 (1959).
8. R. L. ALTMAN, Report UCRL-7044 (1962).
9. T. FUJINO, H. TAGAWA, T. ADACHI, AND H. HASHITANI, submitted for publication.
10. H. ENDO AND M. TANIGUCHI, *Netsu* **1**, 116 (1974).
11. T. L. MARKIN AND R. J. BONES, Report AERE-R-4042 (1962); Report AERE-R-4178 (1962).
12. G. N. LEWIS AND M. RANDALL, "Thermodynamics" (Revised by K. S. Pitzer and Leo Brewer), p. 693, McGraw–Hill, New York (1961).
13. H. NICKEL, *Nukleonik* **8**, 366 (1966).
14. C. KELLER *in* "Gmelins Handbuch der Anorganischen Chemie," Uran, Teil C-3, System No. 55, p. 82, Springer–Verlag, Berlin (1975).
15. P. P. BUDNIKOV, S. G. TRESVYATSKY, AND V. I. KUSHAKOVSKY, *in* "Proceedings of the Second International Conference on the Peaceful Uses of Atomic Energy, Geneva 1958," Vol. 6, p. 124 (1958).
16. M. SUGISAKI, K. HIRASHIMA, S. YOSHIHARA, AND Y. OISHI, *J. Nucl. Sci. Technol.* **10**, 387 (1973).
17. J. B. AINSCOUGH AND F. RIGBY, *J. Inorg. Nucl. Chem.* **36**, 1531 (1974).
18. J. S. ANDERSON AND K. D. B. JOHNSON, *J. Chem. Soc.* 1731 (1953).
19. Y. SAITO, *J. Nucl. Mater.* **51**, 112 (1974).
20. S. ARONSON AND J. C. CLAYTON, *J. Chem. Phys.* **32**, 749 (1960).
21. P. GERDANIAN AND M. DODÉ, *J. Chim. Phys.* **62**, 171 (1965).
22. K. KIUKKOLA, *Acta Chem. Scand.* **16**, 327 (1962).
23. E. STADLBAUER, U. WICHMANN, U. LOTT, AND C. KELLER, *J. Solid State Chem.* **10**, 341 (1974).
24. K. HAGEMARK AND M. BROLI, *J. Amer. Ceram. Soc.* **50**, 563 (1967).